Supplement of Atmos. Chem. Phys. Discuss., 14, 13133–13165, 2014
http://www.atmos-chem-phys-discuss.net/acpd-14-13133-2014/
doi:10.5194/acpd-14-13133-2014-supplement
© Author(s) 2014. CC Attribution 3.0 License.

Atmospheric Chemistry and Physics Discussions

*Supplement of*

# Spatial–temporal variations, sources, and transport of airborne inhalable metals ($PM_{10}$) in urban and rural areas of northern China

**X. S. Luo et al.**

*Correspondence to:* X. D. Li (cexdli@polyu.edu.hk)

**Table captions:**

**Table S1.** Pearson correlation coefficients (r) between concentrations of $PM_{10}$ associated airborne metals (mg $kg^{-1}$) for the warm (N = 105) and cold (N = 105) seasons of seven northern China cities.

**Table S2.** PCA rotated component matrix for concentrations (mg $kg^{-1}$) of trace metals and major elements in the air particles ($PM_{10}$) of different regions (city groups) in northern China.

**Table S3.** Summary of observed values for lead isotope ratios in northern China and some natural background and potential anthropogenic sources in China and Asia.

**Figure captions:**

**Fig. S1.** Trace metal loadings (ng $m^{-3}$) in the warm and cold seasonal $PM_{10}$ of different areas of seven northern Chinese cities (nC, from west to east).

**Fig. S2.** Trace metal concentrations (mg $kg^{-1}$) in the warm and cold seasonal $PM_{10}$ of different areas of seven northern Chinese cities (nC, from west to east).

**Fig. S3.** Temporal variations (warm and cold seasons) in trace metal enrichment factors (EF) in the $PM_{10}$ of different areas of seven northern Chinese cities (nC, from west to east).

**Fig. S4.** Isotopic ratios ($^{206}Pb/^{207}Pb$ vs. $^{208}Pb/^{207}Pb$) for 70 selected aerosol ($PM_{10}$) samples collected in different areas (U-Urban, R-Rural village, B-Rural field) and months of seven cities of northern China from June 2010 to March 2011 compared with natural background and potential anthropogenic sources. The dotted Chinese lead line was drawn using data on major Pb ore deposits and coal in China from references listed in Table S3.

**Fig. S5.** Distributions of cluster-mean five-day backward air mass trajectories (numbers and percentages represent the proportions of each pathway group) with a height of 500 m carried out using a HYSPLIT Model for each city in the sampling cold season (from October 1, 2010 to March 31, 2011), respectively.

**Table S1.** Pearson correlation coefficients (r) between concentrations of $PM_{10}$ associated airborne metals (mg $kg^{-1}$) for the warm (N = 105) and cold (N = 105) seasons of seven northern Chinese cities, respectively.

| | Al | Ca | Cd | Co | **Cu** | Fe | Mg | Ni | Pb | V | Zn |
|---|---|---|---|---|---|---|---|---|---|---|---|
| Al | 1 | **0.89**$^{**}$ | 0.08 | **0.95**$^{**}$ | 0.04 | **0.91**$^{**}$ | **0.97**$^{**}$ | **0.71**$^{**}$ | -0.03 | **0.82**$^{**}$ | 0.07 |
| Ca | **0.78**$^{**}$ | 1 | 0.30$^{**}$ | **0.85**$^{**}$ | 0.18 | **0.87**$^{**}$ | **0.93**$^{**}$ | **0.72**$^{**}$ | 0.20$^{*}$ | **0.75**$^{**}$ | 0.24$^{*}$ |
| Cd | 0.09 | 0.31$^{**}$ | 1 | 0.13 | 0.17 | 0.16 | 0.15 | 0.13 | **0.64**$^{**}$ | 0.24$^{*}$ | 0.47$^{**}$ |
| Co | **0.86**$^{**}$ | **0.63**$^{**}$ | 0.06 | 1 | 0.12 | **0.94**$^{**}$ | **0.93**$^{**}$ | **0.76**$^{**}$ | 0.08 | **0.84**$^{**}$ | 0.16 |
| **Cu** | -0.01 | 0.09 | 0.11 | -0.02 | 1 | 0.20$^{*}$ | 0.08 | 0.30$^{**}$ | 0.37$^{**}$ | 0.13 | 0.31$^{**}$ |
| Fe | **0.77**$^{**}$ | 0.45$^{**}$ | 0.03 | **0.83**$^{**}$ | 0.04 | 1 | **0.90**$^{**}$ | **0.72**$^{**}$ | 0.15 | **0.86**$^{**}$ | 0.20$^{*}$ |
| Mg | **0.95**$^{**}$ | **0.83**$^{**}$ | 0.11 | **0.84**$^{**}$ | -0.02 | **0.70**$^{**}$ | 1 | **0.70**$^{**}$ | 0.03 | **0.81**$^{**}$ | 0.11 |
| Ni | 0.36$^{**}$ | 0.50$^{**}$ | 0.25$^{*}$ | 0.43$^{**}$ | 0.11 | 0.36$^{**}$ | 0.40$^{**}$ | 1 | 0.21$^{*}$ | **0.69**$^{**}$ | 0.15 |
| Pb | -0.00 | 0.21$^{*}$ | **0.69**$^{**}$ | 0.03 | 0.22$^{*}$ | 0.09 | 0.02 | 0.38$^{**}$ | 1 | 0.20$^{*}$ | **0.75**$^{**}$ |
| V | 0.27$^{**}$ | 0.30$^{**}$ | 0.17 | 0.33$^{**}$ | -0.03 | 0.20$^{*}$ | 0.33$^{**}$ | **0.67**$^{**}$ | 0.35$^{**}$ | 1 | 0.20$^{*}$ |
| Zn | -0.14 | 0.04 | **0.62**$^{**}$ | -0.09 | 0.10 | 0.00 | -0.12 | 0.16 | **0.67**$^{**}$ | 0.09 | 1 |

Left: warm season; Wright: cold season.

Significance level: **p < 0.01, *p < 0.05.

**Table S2.** PCA rotated component matrix for concentrations (mg $kg^{-1}$) of trace metals and major elements in the air particles ($PM_{10}$) of different regions (city groups) in northern China.

| | WW-YC-TY (n=105) | | BJ-DZ (n=47) | | | YT-DL (n=58) | | |
|---|---|---|---|---|---|---|---|---|
| | PC1 | PC2 | PC1 | PC2 | PC3 | PC1 | PC2 | PC3 |
| Al | **0.98** | -0.03 | **0.93** | -0.09 | 0.19 | **0.97** | 0.04 | 0.13 |
| Ca | **0.83** | 0.39 | **0.90** | 0.28 | -0.06 | **0.89** | 0.03 | 0.24 |
| Cd | 0.15 | **0.91** | 0.18 | **0.84** | -0.15 | **0.54** | **0.53** | 0.09 |
| Co | **0.97** | 0.02 | **0.88** | -0.06 | 0.39 | **0.80** | 0.27 | 0.19 |
| Cu | -0.02 | **0.51** | 0.25 | 0.03 | **0.84** | -0.03 | **0.59** | 0.27 |
| Fe | **0.96** | 0.02 | **0.93** | -0.05 | 0.25 | **0.52** | **0.57** | -0.28 |
| Mg | **0.97** | -0.01 | **0.95** | -0.10 | 0.08 | **0.94** | 0.06 | 0.19 |
| Ni | **0.62** | 0.42 | 0.07 | 0.12 | **0.73** | 0.39 | 0.14 | **0.83** |
| Pb | 0.00 | **0.94** | -0.03 | **0.90** | 0.16 | 0.10 | **0.81** | 0.15 |
| V | **0.97** | -0.05 | **0.67** | 0.21 | -0.01 | 0.16 | 0.02 | **0.93** |
| Zn | 0.07 | **0.73** | -0.05 | **0.88** | 0.18 | 0.10 | **0.87** | -0.18 |
| Eigenvalue (>1) | 5.98 | 2.68 | 5.10 | 2.46 | 1.28 | 4.94 | 2.02 | 1.40 |
| % of Variance | 54.4 | 24.3 | 46.4 | 22.4 | 11.6 | 44.9 | 18.4 | 12.8 |
| Cumulative % | 54.4 | 78.7 | 46.4 | 68.8 | 80.4 | 44.9 | 63.3 | 76.0 |
| Main sources | Crustal (soil/dust) | Coal combustion /Traffic | Crustal | Coal combustion /Traffic | Metallurgical industry | Crustal | Coal combustion /Traffic | Petrochemical industry, oil combustion |

Factor loading values ≥0.50 are highlighted and in bold font.

**Table S3.** Summary of observed values for lead isotope ratios in northern China and some natural background and potential anthropogenic sources in China and Asia.

| Matrix | Pb (mg kg$^{-1}$) | $^{206}Pb/^{207}Pb$ | $^{208}Pb/^{207}Pb$ | $^{204}Pb/^{207}Pb$ | Reference |
|---|---|---|---|---|---|
| $PM_{10}$ nC-U (34) | 806 | 1.1581 | 2.4507 | 0.06415 | |
| | (137-1740) | (1.1136-1.1785) | (2.4181-2.4702) | (0.06371-0.06459) | This study |
| $PM_{10}$ nC-R (18) | 569 | 1.1498 | 2.4463 | 0.06435 | |
| | (197-1297) | (1.1020-1.1687) | (2.4160-2.4632) | (0.06388-0.06502) | |
| $PM_{10}$ nC-B (18) | 882 | 1.1520 | 2.4450 | 0.06420 | |
| | (317-1496) | (1.1053-1.1660) | (2.4103-2.4597) | (0.06389-0.06469) | |
| ***Natural sources (soil)*** | | | | | (Ferrat et al., 2012) |
| Northwestern China | 39.3 | 1.195 | 2.480 | 0.06383 | |
| Northern China | 22.0 | 1.196 | 2.485 | 0.06383 | |
| | (14.1-37.3) | (1.184-1.202) | (2.474-2.490) | (0.06379-0.06391) | |
| Tibetan Plateau | 24.2 | 1.196 | 2.490 | 0.06376 | |
| India | 18.6 | 1.239 | 2.522 | 0.06306 | |
| ***Anthropogenic sources*** | | | | | |
| *Vehicular emissions* | | | | | |
| Shanghai vehicle exhaust (leaded) | 7804 ± 160 | 1.1100 | 2.4351 | | (Tan et al., 2006) |
| Shanghai vehicle exhaust (lead free) | 238 ± 5 | 1.1474 | 2.4372 | | (Tan et al., 2006) |
| PRD automobile exhaust | | 1.1604 | 2.4228 | 0.06420 | (Zhu et al., 2001) |
| *Coal combustion* | | | | | (Cheng and Hu, 2010) |
| Northern Chinese coal | | 1.1781 | 2.4748 | | (Mukai et al., 1993) |
| Chinese coal | 22 | 1.1546 | 2.4534 | | (Diaz-Somoano et al., 2009) |
| Coal used in Shanghai | | 1.1628 | 2.4616 | | (Liang et al., 2010) |
| Coal combustion in Shanghai | 1788 ± 37 | 1.1633 | 2.4559 | | (Tan et al., 2006) |
| *Metallurgic dust (Shanghai)* | 6140 ± 130 | 1.1725 | 2.4350 | | (Tan et al., 2006) |
| *Cement (Shanghai)* | 103 ± 2 | 1.1631 | 2.4466 | | (Tan et al., 2006) |
| *Chinese Pb ore deposit* | | 1.0259-1.1809 | 2.3168-2.4751 | 0.06388-0.06592 | (Zhu et al., 2010; Cheng and Hu, 2010) |

nC-northern China; U-urban, R-rural village, B-rural field.

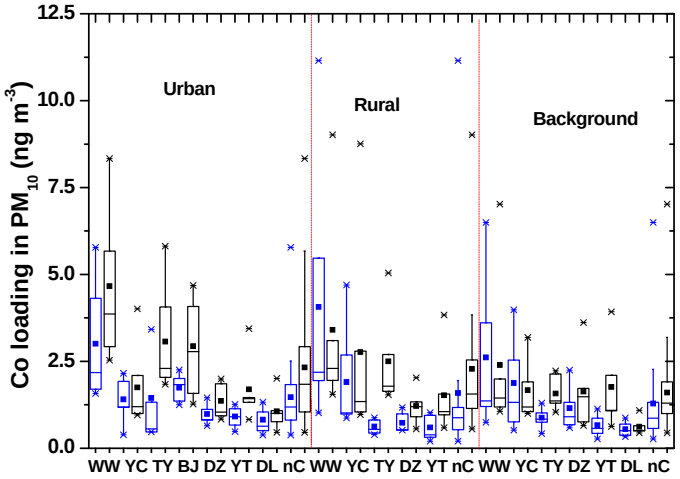
Co loading in PM10 (ng m-3)
12.5
10.0
7.5
5.0
2.5
0.0
Urban
Rural
Background
WW YC TY BJ DZ YT DL nC WW YC TY DZ YT nC WW YC TY DZ YT DL nC

59

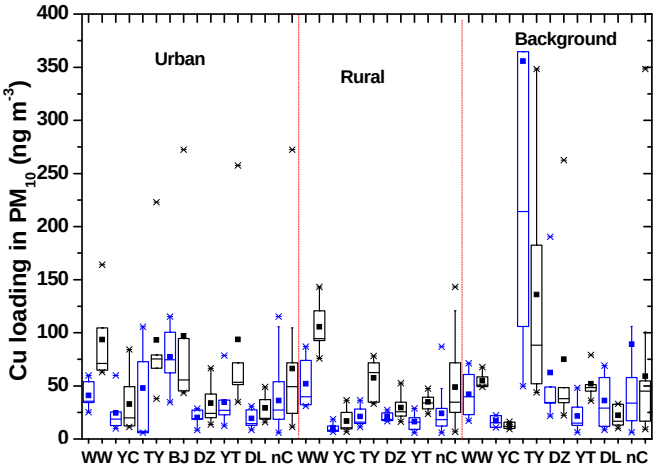
Cu loading in PM10 (ng m-3)
400
350
300
250
200
150
100
50
0
Urban
Rural
Background
WW YC TY BJ DZ YT DL nC WW YC TY DZ YT nC WW YC TY DZ YT DL nC

60

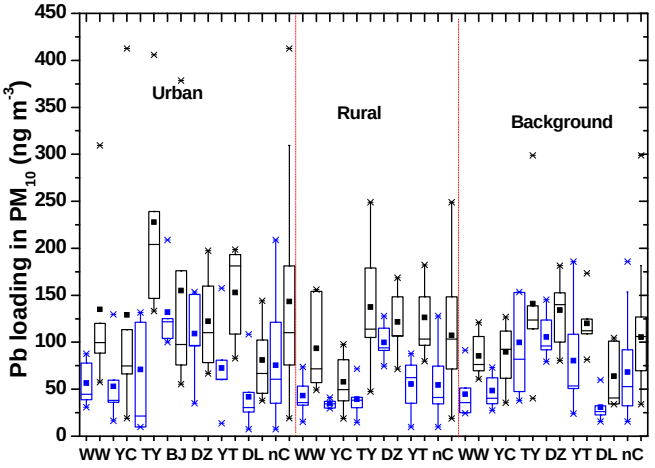
Pb loading in PM10 (ng m-3)
450
400
350
300
250
200
150
100
50
0
Urban
Rural
Background
WW YC TY BJ DZ YT DL nC WW YC TY DZ YT nC WW YC TY DZ YT DL nC

61

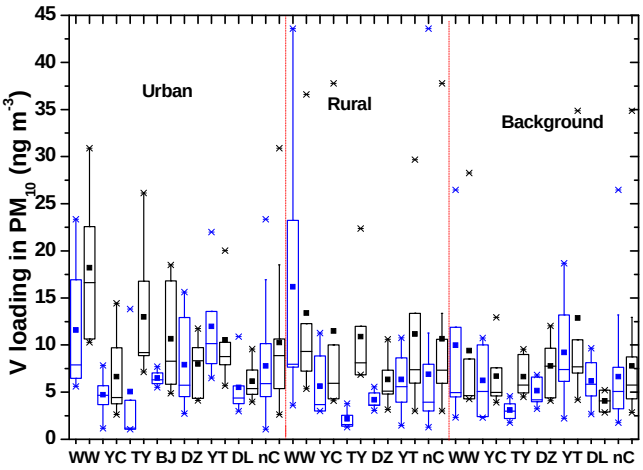


62

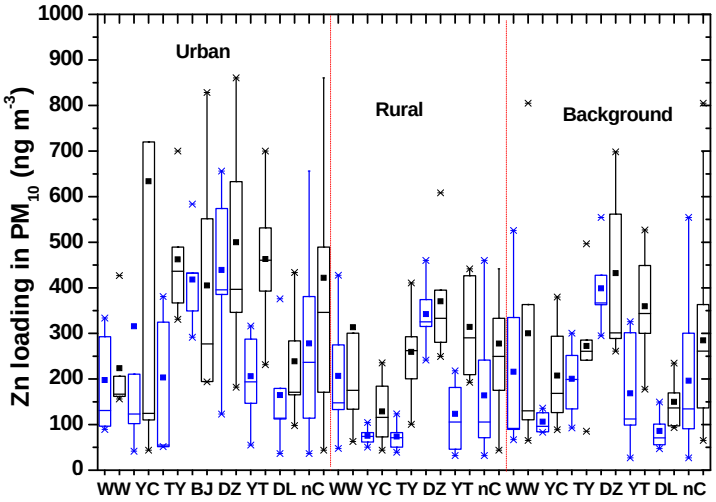


63

64 **Fig. S1.** Trace metal loadings (ng $m^{-3}$) in the warm and cold seasonal $PM_{10}$ of different areas of
65 seven northern Chinese cities (nC, from west to east).

66

67

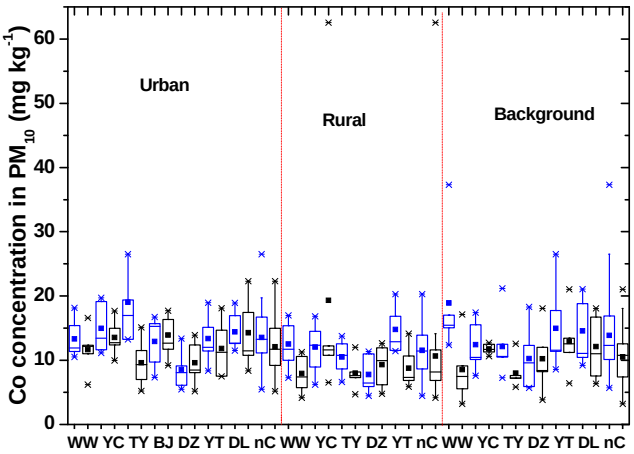
Co concentration in PM10 (mg kg-1)
Urban
Rural
Background
WW YC TY BJ DZ YT DL nC WW YC TY DZ YT nC WW YC TY DZ YT DL nC

68

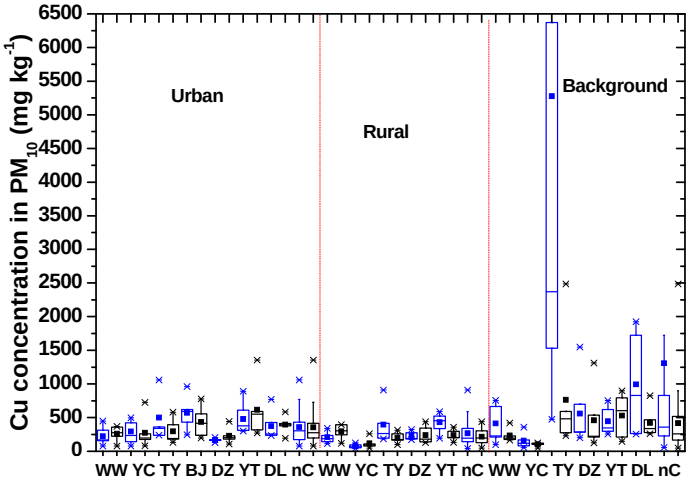
Cu concentration in PM10 (mg kg-1)
Urban
Rural
Background
WW YC TY BJ DZ YT DL nC WW YC TY DZ YT nC WW YC TY DZ YT DL nC

69

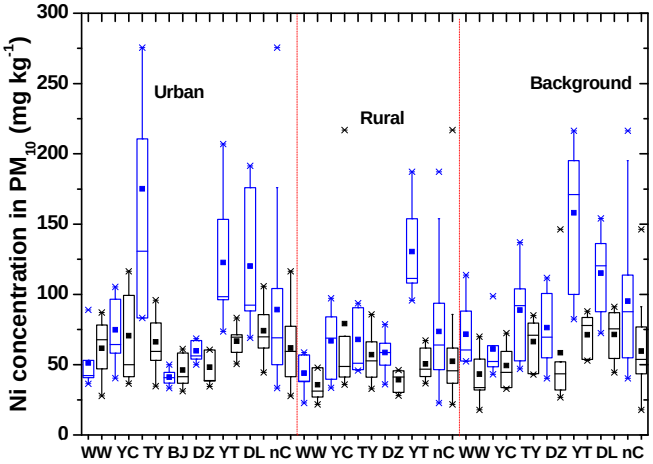
Ni concentration in PM10 (mg kg-1)
Urban
Rural
Background
WW YC TY BJ DZ YT DL nC WW YC TY DZ YT nC WW YC TY DZ YT DL nC

70

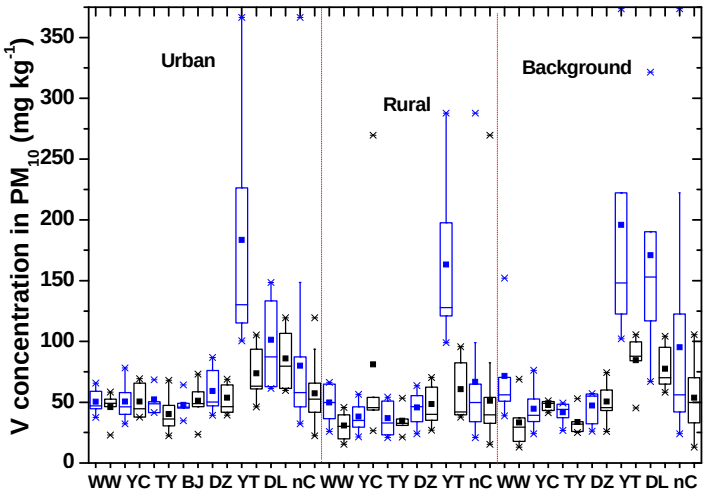


71

72 **Fig. S2.** Trace metal concentrations (mg $kg^{-1}$) in the warm and cold seasonal $PM_{10}$ of different
73 areas of seven northern Chinese cities (nC, from west to east).

74

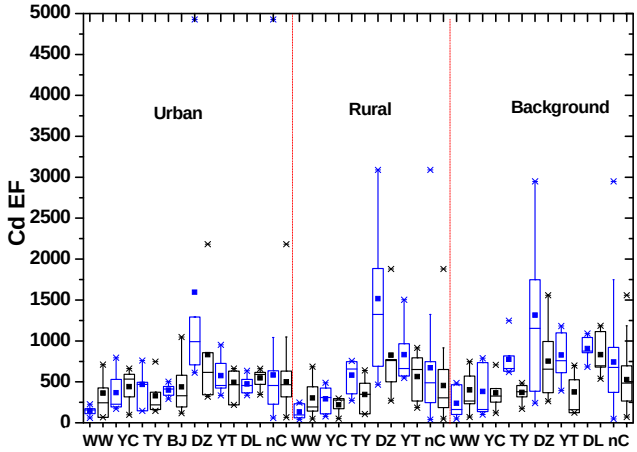
Cd EF
Urban
Rural
Background
WW YC TY BJ DZ YT DL nC WW YC TY DZ YT nC WW YC TY DZ YT DL nC

75

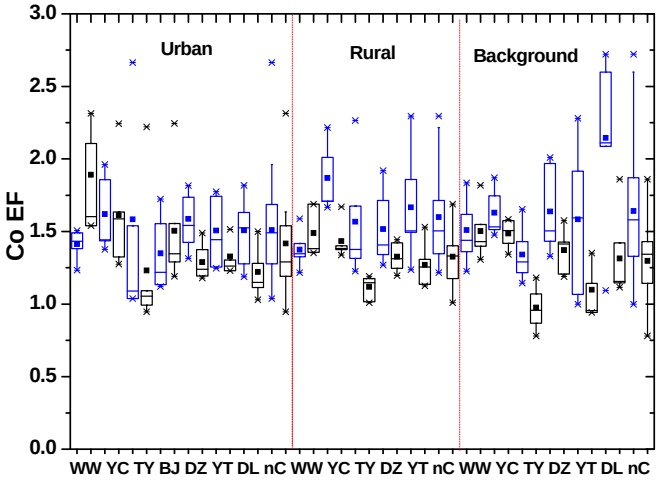
Co EF
Urban
Rural
Background
WW YC TY BJ DZ YT DL nC WW YC TY DZ YT nC WW YC TY DZ YT DL nC

76

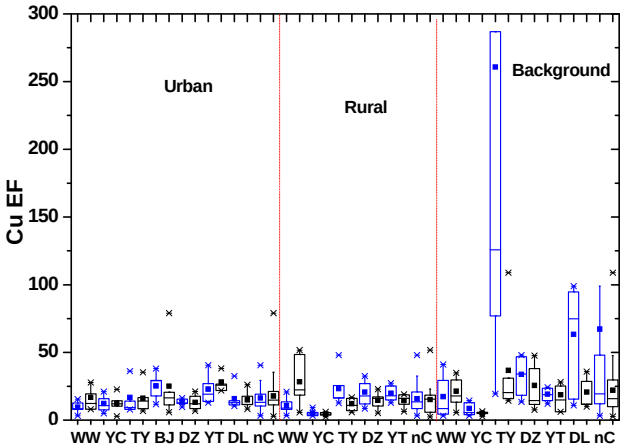
Cu EF
Urban
Rural
Background
WW YC TY BJ DZ YT DL nC WW YC TY DZ YT nC WW YC TY DZ YT DL nC

77

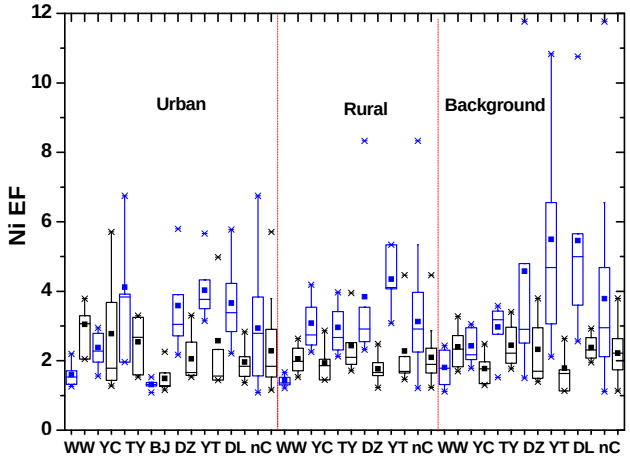
Ni EF
Urban
Rural
Background
0
2
4
6
8
10
12
WW YC TY BJ DZ YT DL nC WW YC TY DZ YT nC WW YC TY DZ YT DL nC

78

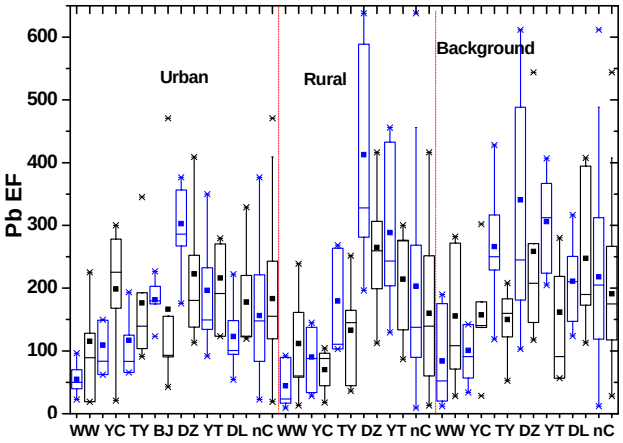
Pb EF
Urban
Rural
Background
0
100
200
300
400
500
600
WW YC TY BJ DZ YT DL nC WW YC TY DZ YT nC WW YC TY DZ YT DL nC

79

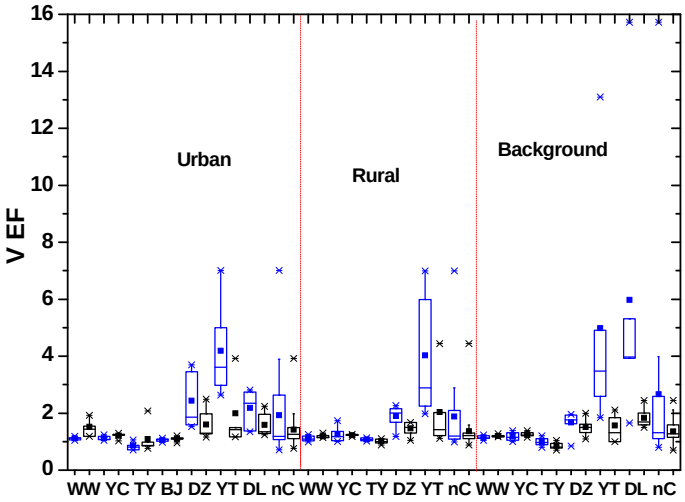
V EF
Urban
Rural
Background
0
2
4
6
8
10
12
14
16
WW YC TY BJ DZ YT DL nC WW YC TY DZ YT nC WW YC TY DZ YT DL nC

80

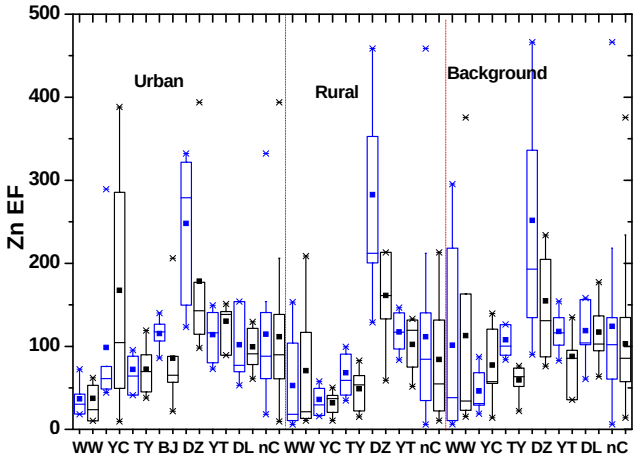


**Fig. S3.** Temporal variations (warm and cold seasons) in trace metal enrichment factors (EF) in the $PM_{10}$ of different areas of seven northern Chinese cities (nC, from west to east).

85

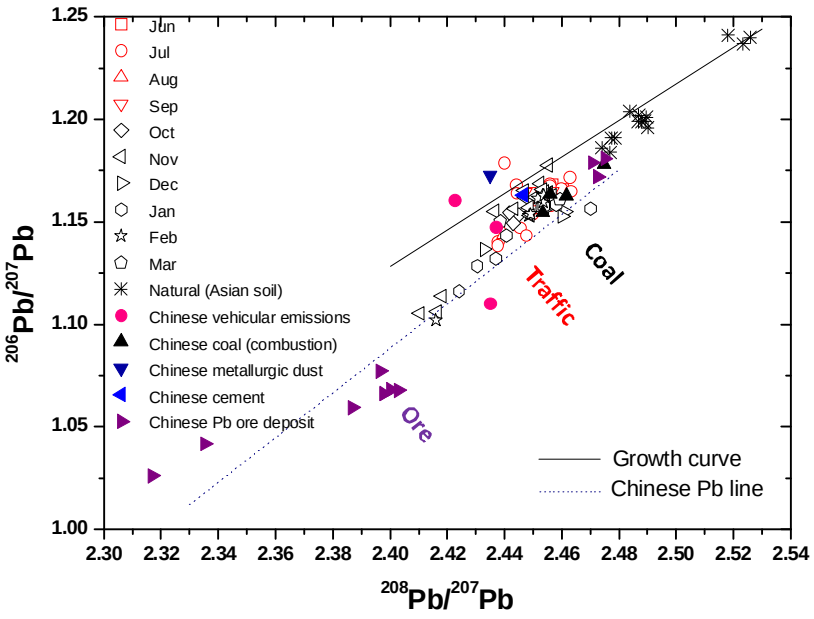
Jun
Jul
Aug
Sep
Oct
Nov
Dec
Jan
Feb
Mar
Natural (Asian soil)
Chinese vehicular emissions
Chinese coal (combustion)
Chinese metallurgic dust
Chinese cement
Chinese Pb ore deposit
Traffic
Coal
Ore
Growth curve
Chinese Pb line
$^{206}Pb/^{207}Pb$
$^{208}Pb/^{207}Pb$

86

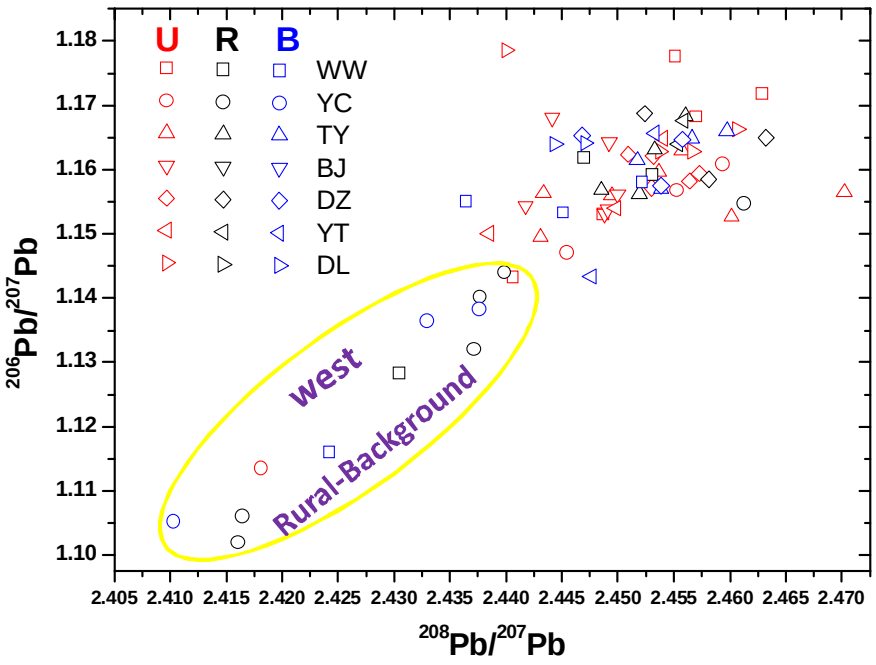
U
R
B
WW
YC
TY
BJ
DZ
YT
DL
west
Rural-Background
$^{206}Pb/^{207}Pb$
$^{208}Pb/^{207}Pb$

87

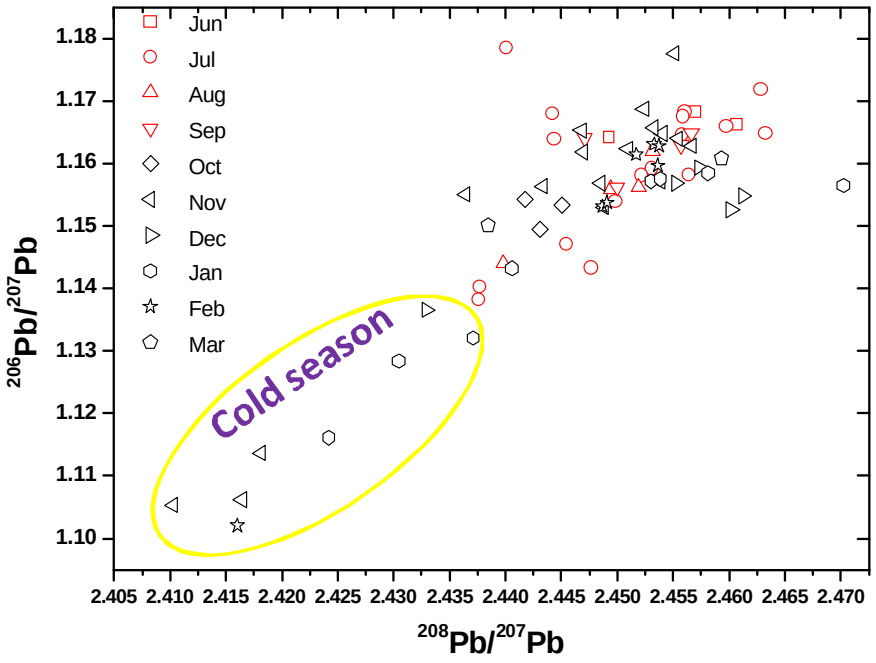


88

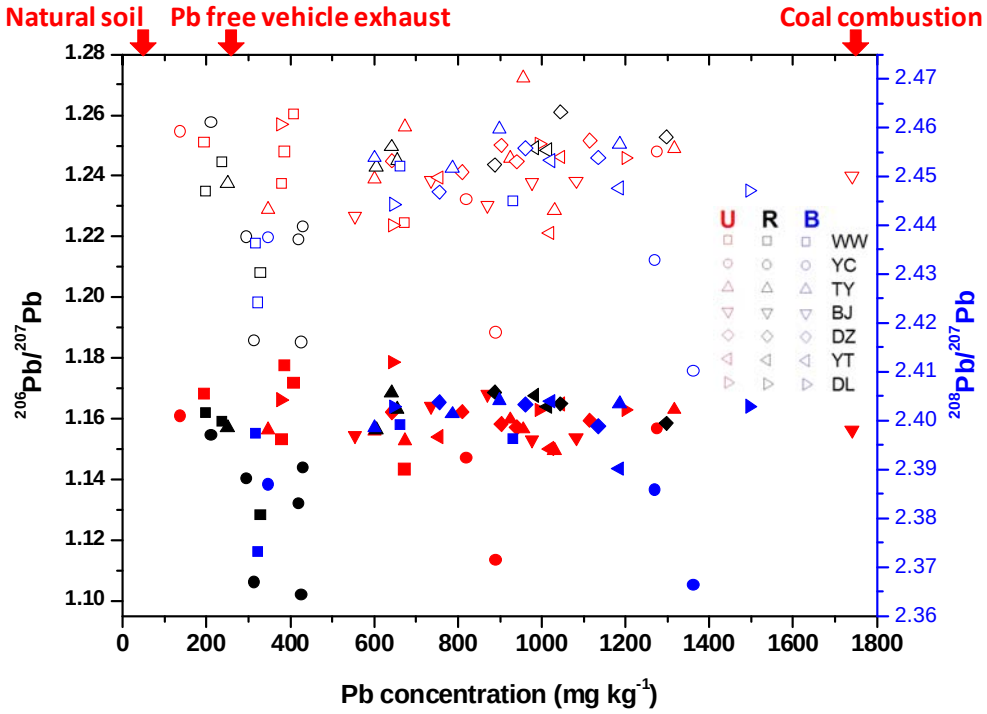


89

90 **Fig. S4.** Isotopic ratios ($^{206}Pb/^{207}Pb$ vs. $^{208}Pb/^{207}Pb$) for 70 selected aerosol ($PM_{10}$) samples
91 collected in different areas (U-Urban, R-Rural village, B-Rural field) and months of seven cities in
92 northern China from June 2010 to March 2011 compared with natural background and potential
93 anthropogenic sources. The dotted Chinese lead line was drawn using data on major Pb ore
94 deposits and coal in China from references listed in Table S3.

95

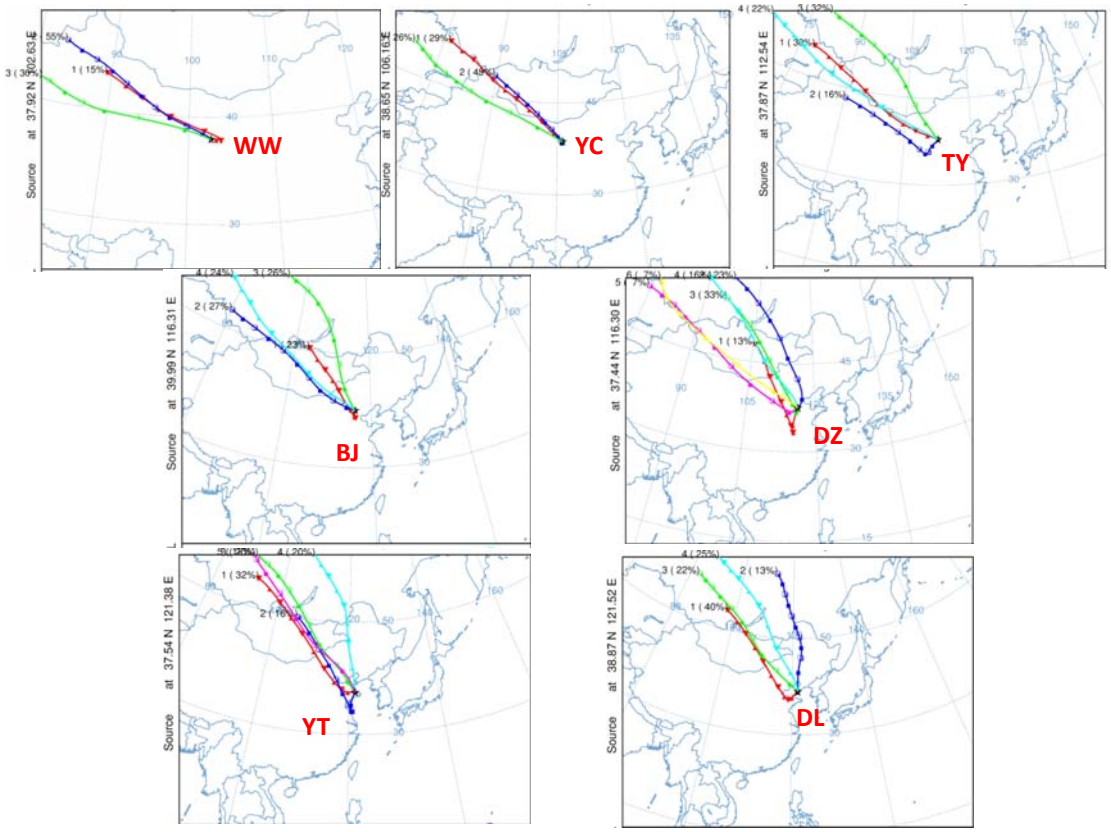


**Fig. S5.** Distributions of cluster-mean five-day backward air mass trajectories (numbers and percentages represent the proportions of each pathway group) with a height of 500 m carried out using a HYSPLIT Model for each city in the sampling cold season (from October 1, 2010 to March 31, 2011), respectively.

## References


Cheng, H. F., and Hu, Y. A.: Lead (Pb) isotopic fingerprinting and its applications in lead pollution studies in China: A review, Environ. Pollut., 158, 1134-1146, 2010.

Diaz-Somoano, M., Kylander, M. E., Lopez-Anton, M. A., Suarez-Ruiz, I., Martinez-Tarazona, M. R., Ferrat, M., Kober, B., and Weiss, D. J.: Stable Lead Isotope Compositions In Selected Coals From Around The World And Implications For Present Day Aerosol Source Tracing, Environ. Sci. Technol., 43, 1078-1085, 10.1021/es801818r, 2009.

Ferrat, M., Weiss, D. J., Dong, S. F., Large, D. J., Spiro, B., Sun, Y. B., and Gallagher, K.: Lead atmospheric deposition rates and isotopic trends in Asian dust during the last 9.5 kyr recorded in an ombrotrophic peat bog on the eastern Qinghai-Tibetan Plateau, Geochim. Cosmochim. Acta., 82, 4-22, 2012.

Liang, F., Zhang, G. L., Tan, M. G., Yan, C. H., Li, X. L., Li, Y. L., Li, Y., Zhang, Y. M., and Shan, Z. C.: Lead in Children's Blood Is Mainly Caused by Coal-Fired Ash after Phasing out of Leaded Gasoline in Shanghai, Environ. Sci. Technol., 44, 4760-4765, 2010.

Mukai, H., Furuta, N., Fujii, T., Ambe, Y., Sakamoto, K., and Hashimoto, Y.: Characterization of Sources of Lead in the Urban Air of Asia Using Ratios of Stable Lead Isotopes, Environ. Sci. Technol., 27, 1347-1356, 1993.

Tan, M. G., Zhang, G. L., Li, X. L., Zhang, Y. X., Yue, W. S., Chen, J. M., Wang, Y. S., Li, A. G., Li, Y., Zhang, Y. M., and Shan, Z. C.: Comprehensive study of lead pollution in Shanghai by multiple techniques, Anal. Chem., 78, 8044-8050, 2006.

Zhu, B. Q., Chen, Y. W., and Peng, J. H.: Lead isotope geochemistry of the urban environment in the Pearl River Delta, Appl. Geochem., 16, 409-417, 2001.

Zhu, L. M., Tang, J. W., Lee, B., Zhang, Y., and Zhang, F. F.: Lead concentrations and isotopes in aerosols from Xiamen, China, Mar. Pollut. Bull., 60, 1946-1955, 10.1016/j.marpolbul.2010.07.035, 2010.